

The ClO amounts derived here are sensitive to systematic errors in the retrieved column O<sub>3</sub> amounts (22). It has been suggested that TOMS may underestimate O<sub>3</sub> near the terminator. If so, the O<sub>3</sub> loss in the vortex during September—and thus the ClO concentrations—could be greater than computed here. This error implies that ClO concentrations near the center of the O<sub>3</sub> hole were greater than the values that have yet been observed at the more equatorward (equivalent) latitudes reached by the AAOE aircraft.

#### REFERENCES AND NOTES

1. J. C. Farman, B. G. Gardiner, J. D. Shanklin, *Nature* **315**, 207 (1985).
2. The discovery (1) was confirmed by R. S. Stolarski *et al.*, *ibid.* **322**, 808 (1986), using TOMS satellite data.
3. S. Solomon, R. R. Garcia, F. S. Rowland, D. J. Wuebbles, *ibid.* **321**, 755 (1986); M. B. McElroy, R. J. Salawitch, S. C. Wofsy, J. A. Logan, *ibid.*, p. 759; L. T. Molina and M. J. Molina, *J. Phys. Chem.* **91**, 433 (1986).
4. The results of the AAOE are summarized in R. Watson, B. Toon, A. Tuck, Eds., *J. Geophys. Res.* **94**, 11179 (1989); *ibid.*, p. 16437.
5. J. G. Anderson *et al.*, *ibid.*, p. 11465; *ibid.*, p. 11480.
6. J. W. Barrett *et al.*, *Nature* **336**, 455 (1988).
7. S. P. Sander, R. R. Friedl, Y. L. Yung, *Science* **245**, 1095 (1989).
8. R. S. Stolarski and M. R. Schoeberl, *Geophys. Res. Lett.* **13**, 1210 (1986); M. R. Schoeberl, A. J. Krueger, P. A. Newman, *ibid.*, p. 1217.
9. The idea of area mapping of Ertel's potential vorticity on an isentropic surface was first suggested by M. E. McIntyre and T. N. Palmer [*J. Atmos. Terr. Phys.* **46**, 825 (1984)] and fruitfully used by N. Butchart and E. E. Remsberg [*J. Atmos. Sci.* **43**, 1319 (1986)] for studying the northern polar vortex. We have not used Ertel's potential vorticity because of the lack of high-quality dynamical data. Instead we used column O<sub>3</sub>,  $\Omega$ , as a proxy for a conservative tracer.
10. A. J. Krueger *et al.*, *The 1987 Airborne Antarctic Ozone Experiment* (NASA Ref. Publ. 1201, National Aeronautics and Space Administration, Washington, DC, 1988).
11. The difference between the zonal mean O<sub>3</sub> and the area-mapped O<sub>3</sub> can be used as a measure of the effective displacement of the vortex off the pole.
12. For instance, the original McMurdo data show that, from day 240 to day 278, O<sub>3</sub> has apparently decreased by about 120 DU. The area-mapped data indicate that the loss at  $\theta_E = -78^\circ$  is only about 70 DU. The remaining 50 DU is caused by displacements of the vortex center. This difference can be significant in a comparison of data and theory. Not only is the loss of 70 DU during this period more compatible with existing chemical theories, but also the shape of the loss profile—slower rate in the early period (when the number of sunlight hours is small) and faster rate later (when the day becomes longer)—is more consistent with these theories (5, 7). The model of Sander *et al.* (7) can account for the O<sub>3</sub> loss rates at  $\theta_E = -78^\circ$ , whereas it has difficulties with the original McMurdo data.
13. We first performed a 9-day weighted averaging of the data to get rid of the daily fluctuations. The relative weighting for the central date is 1 and is 0.8, 0.6, 0.4, and 0.2, respectively, for points  $\pm 1, \pm 2, \pm 3$ , and  $\pm 4$  days away from the central date. A comparison of the original and smoothed data indicates that all the large-scale features of interest are preserved in the smoothing. We have also tried filtering with boxcar windows of 3, 5, 7, and 9 days. The essential features are preserved.
14. The differentiation is carried out by differencing the smoothed data points separated by 1 day. Because of the smoothing described in (13), the derived  $\partial\Omega/\partial t$  represents O<sub>3</sub> losses averaged over several days.
15. It is generally accepted that the catalytic mechanisms for destroying O<sub>3</sub> are ineffective by this time. S. Solomon *et al.*, *J. Geophys. Res.* **94**, 11393 (1989); R. W. Sanders *et al.*, *ibid.*, p. 11381; C. B. Farmer *et al.*, *Nature* **329**, 126 (1987).
16. K. K. Tung, M. K. W. Ko, J. M. Rodriguez, N. D. Sze, *Nature* **333**, 811 (1986).
17. J. D. Mahlman and S. B. Fels, *Geophys. Res. Lett.* **13**, 1316 (1986).
18. At  $z = 18$  km on day 255 (12 September),  $S = 12$  hours at all latitudes. Before this date  $S < 12$  hours and after this date  $S > 12$  hours. The pole at 18 km remains in the shadow before day 250 (7 September) and starts to receive more than 20 hours of sunlight per day after day 260 (17 September).  $S$  can be readily computed as a function of latitude, altitude, and time. However, we consider the computation of a static  $S$  based on geometry and solar illumination alone as unrealistic, because each parcel of air moves around the pole and makes large excursions across latitude circles. Thus, the correct  $S$  must reflect the trajectory history of any air parcel. Because the O<sub>3</sub> isopleths are approximately the trajectories of air parcels in the vortex, we can derive an approximate trajectory-averaged number of sunlight hours per day,  $\bar{S}$ , by performing the appropriate weighting around each O<sub>3</sub> contour. The general behavior of  $\bar{S}$  is consistent with excursions of the vortex off the pole; thus, the number of hours of exposure to sunlight in early spring increased relative to the zonal mean value.
19. We used the model of Sander *et al.* (7) without the higher chlorine oxides and with the effective length of the day  $\bar{S}$  computed in (18). We adopted the vertical profile of ClO obtained by Barrett *et al.* (6). On day 260, ClO = 1.1 ppbv at 18 km,  $\bar{S} = 15$  hours at McMurdo ( $A = 0.0219 \times 2\pi R^2$ ,  $\theta_E = -78^\circ$ ),  $\partial\Omega/\partial t = -2.5$  DU per day. We deduced all other values of ClO at 18 km by inverting Eq. 5 without the dynamical term and holding the concentrations of BrO and HO<sub>2</sub> fixed as in (7).
20. W. H. Brune, D. W. Toohey, J. G. Anderson, *Eos* **70**, 1040 (1989).
21. R. L. de Zafra *et al.*, *J. Geophys. Res.* **94**, 11423 (1989).
22. It is known that TOMS measurements tend to underestimate total column O<sub>3</sub> abundances by 20 to 40 DU near the terminator. This error implies that the actual initial O<sub>3</sub> abundances near the vortex center are higher than the values reported here. Hence the loss rates would be higher also.
23. We are grateful to R. Stolarski for providing TOMS data before publication and to P. Newman for sending us potential vorticity data. We thank K. K. Tung, R. Friedl, J. Rodriguez, M. Schoeberl, and R. L. Shia for illuminating discussions, S. Solomon for critical comments on systematic errors of TOMS data, and X.-L. Zhu for plotting all the graphs in this report. Part of the research described in this paper was carried out by the Jet Propulsion Laboratory, under contract with the National Aeronautics and Space Administration, and was also supported by NASA grant NAGW-413 to the California Institute of Technology. Contribution number 4783 from the Division of Geological and Planetary Sciences, California Institute of Technology.

24 October 1989; accepted 22 February 1990

## A Genetic Test of the Natal Homing Versus Social Facilitation Models for Green Turtle Migration

ANNE B. MEYLAN, BRIAN W. BOWEN, JOHN C. AVISE

Female green turtles exhibit strong nest-site fidelity as adults, but whether the nesting beach is the natal site is not known. Under the natal homing hypothesis, females return to their natal beach to nest, whereas under the social facilitation model, virgin females follow experienced breeders to nesting beaches and after a "favorable" nesting experience, fix on that site for future nestings. Differences shown in mitochondrial DNA genotype frequency among green turtle colonies in the Caribbean Sea and Atlantic Ocean are consistent with natal homing expectations and indicate that social facilitation to nonnatal sites is rare.

**M**ARINE TURTLES OFTEN USE nesting beaches that are hundreds or even thousands of kilometers removed from their foraging grounds. The hypothesis that marine turtles return to nest on their natal beach (perhaps guided in part by olfaction) (1) is derived primarily from the strong nest-site fidelity of adult females, as revealed by repeated capture of tagged individuals on the same beach in successive nesting seasons (2–7). Despite the fundamental importance of this possibility to an understanding of turtle life histories, the

natal homing hypothesis remains unproven. The main obstacle to testing it has been the lack of a physical tag that persists on a turtle for the estimated 30 or more years that elapse between hatching and sexual maturation (8). Colonial nesting and nest-site fidelity are known to be especially well developed in the green turtle (*Chelonia mydas*) (2, 3, 4, 7); only in rare instances (9, 10) have marked adult females been observed at a nesting beach other than the one at which they were originally tagged.

Hendrickson (11) and Owens *et al.* (12) advanced an alternative theory for nest-site selection that is also consistent with the observed site fidelity of adult females. Under their social facilitation model, virgin (mature, unmated) females randomly encounter experienced females on foraging grounds. They then follow the experienced females to

A. B. Meylan, Department of Natural Resources, Florida Marine Research Institute, 100 Eighth Avenue, S.E., St. Petersburg, FL 33701, and Department of Herpetology and Ichthyology, American Museum of Natural History, New York, NY 10024.  
B. W. Bowen and J. C. Avise, Department of Genetics, University of Georgia, Athens, GA 30602.

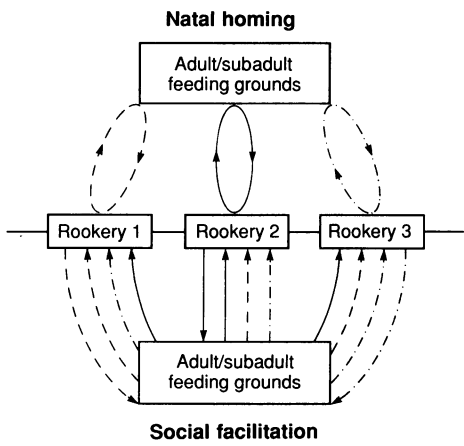


**Fig. 1.** Schematic representation of the single-generation migratory circuits (hatchlings to subadult/adult feeding grounds to nesting beaches) expected under the natal homing versus social facilitation scenarios of female green turtle movement. Under the natal homing hypothesis (upper half of figure), the closed migratory circuit between each rookery and the foraging grounds implies no mtDNA gene flow between nesting beaches; under the social facilitation hypothesis (lower half of figure), the open migratory circuits imply extensive mtDNA gene flow between rookeries.

a nesting beach and after having a “favorable” nesting experience, fix on that site for future nestings.

When females from different nesting colonies share foraging grounds, expectations regarding the geographic distribution of maternally transmitted mitochondrial DNA (mtDNA) genotypes at the nesting beaches

are distinctly different under the natal homing and social facilitation models (Fig. 1). If female turtles return faithfully to their natal beach to nest, maternal lineages in different colonies should evolve independently from one another and accumulate mtDNA differences over time. Alternatively, under the social facilitation model, exchange of lineages among nesting colonies should result in considerable mtDNA gene flow among colonies.

For the genetic test reported here of the natal homing versus social facilitation hypotheses, green turtle populations in the Caribbean Sea and Atlantic Ocean were selected because they have been extensively studied (1, 4, 13–15), migration patterns in the area are well documented, and turtles from at least two nesting beaches overlap on numerous foraging grounds (Fig. 2). Restriction site analysis of mtDNA was used because of its proven sensitivity in revealing geographic population structure in other animals (16–19). The maternal mode of inheritance makes mtDNA especially appropriate for studies of female natal homing in marine turtles because the effects of male migratory behavior do not confound mtDNA phylogeographic patterns.

Sample sizes and localities (Table 1) were dictated largely by permit limitations on this endangered species. Laboratory methods are described elsewhere (20–22). Fourteen informative restriction enzymes were used in the mtDNA digestions: Ava II, Bcl I, Dde I, Eco RI, Eco RV, Hinc II, Hind III, Mbo I,

Msp I, Nde I, Pvu II, Spe I, Sst II, and Stu I (23). All changes in mtDNA fragment profiles on gels could be accounted for by specific restriction site gains or losses. Thus genetic distances (base substitutions per nucleotide) between mtDNA genomes were estimated by the site approach (24).

In terms of nucleotide sequence, the mtDNAs from the four nesting colonies appear highly similar, sharing at least 96 of the approximately 98 restriction sites scored per individual. Among the 49 assayed turtles, only three different mtDNA genotypes (hereafter denoted A, B, and C) were observed. The sequence divergences estimated between genotype pairs A-B, A-C, and B-C were  $P = 0.002$ ,  $P = 0.001$ , and  $P = 0.001$ , respectively. In our assays, genotype A differed from C by a single Spe I site loss; B differed from C by a single Hinc II site gain; and A differed from B by these two restriction sites [see figure 2 of (24)].

In terms of mtDNA genotype frequencies, however, three of the four rookeries were distinct (Tables 1 and 2). Ascension Island appeared fixed for genotype C, which was observed at no other locality; Aves Island exhibited in high frequency (87%) the genotype B, which was not seen elsewhere. Only the Florida and Tortuguero samples were indistinguishable in our assays.

Slatkin and Maddison [(25), see also (26)] recently introduced a method for estimating gene flow between populations based on the minimum number of migration events nec-

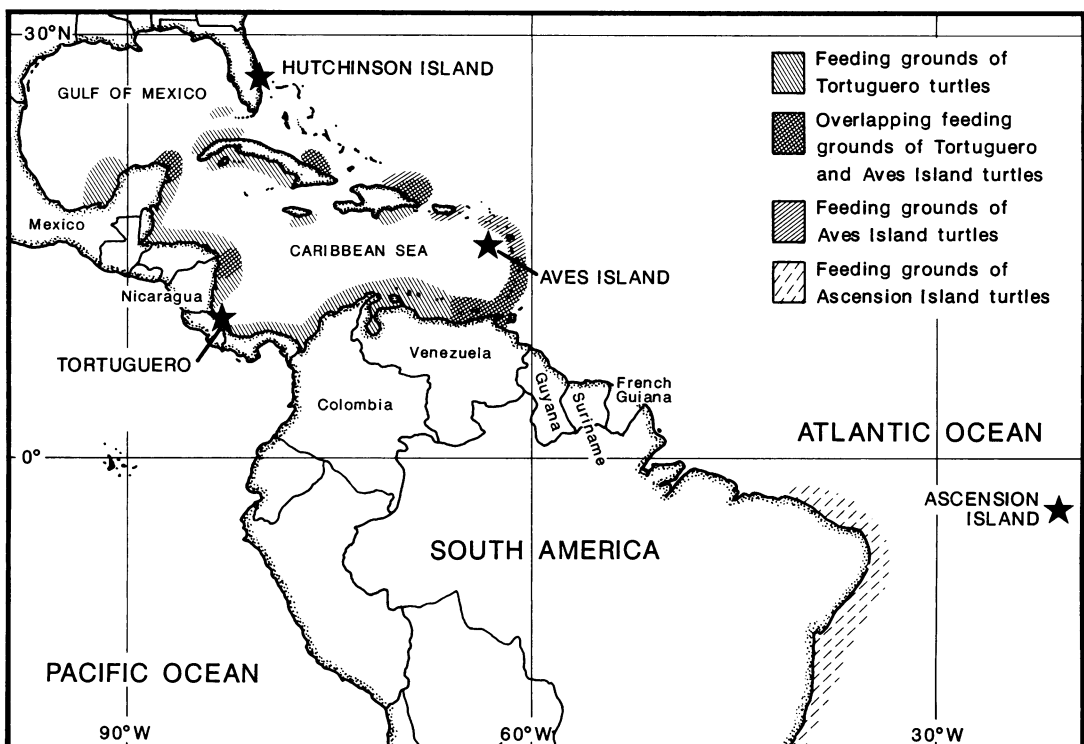


**Fig. 2.** Map of the Caribbean and Western Central Atlantic Ocean showing the foraging grounds used by green turtles that nest at three of the four surveyed rookeries (the foraging grounds of the Florida colony are unknown). Information on the foraging grounds is derived from (6, 13, 14, 30).

**Table 1.** Numbers of individuals showing mtDNA genotypes A, B, and C at the four green turtle rookeries. Significant heterogeneity in genotype frequency exists among locales ( $G_H = 90.0$ ,  $P < 0.005$ ).

Location	MtDNA genotypes		
	A	B	C
Aves Island (Venezuela)	1	7	0
Tortuguero (Costa Rica)	15	0	0
Ascension Island (U.K.)	0	0	16
Hutchinson Island, FL (U.S.A.)	10	0	0

essary to account for an observed geographic distribution of mtDNA haplotypes whose phylogenetic relationships are known or hypothesized. The approach yields an estimate of  $Nm$ , where  $N$  is the size of each local population and  $m$  is the migration rate. In general, values of  $Nm$  much greater than 1 indicate that gene flow (or historical associations among populations, or both) have been sufficient to prevent substantial divergence at neutral loci by genetic drift. The results of the Slatkin-Maddison approach as applied to our data (Table 2) strongly support the contention that female-mediated gene flow between the assayed rookeries (with the possible exception of Tortuguero-Florida) has been rare.

The geographic distribution of mtDNA genotypes is largely consistent with expectations of the natal homing hypothesis and appears to be at odds with predictions of the social facilitation model. Nonetheless, several caveats should be considered before this conclusion is accepted in unqualified form.

First, the foraging grounds associated with the Ascension colony are not known to overlap with those of the other colonies studied. Thus, mtDNA gene flow between Ascension and the other nesting beaches could be limited primarily by natal homing

on a regional geographic scale, rather than lack of social facilitation between adjacent rookeries.

Second, we were unable to distinguish the Florida and Tortuguero samples in our mtDNA analyses (Table 1). Although this might be attributable to high, continuous gene flow (as under the social facilitation model), alternative explanations can also be advanced: (i) perhaps more refined tests would reveal genotypic differences between Florida and Tortuguero turtles; or (ii) perhaps the Florida rookery has been established very recently by turtles carrying Tortuguero-like mtDNAs (15). A confounding factor for the Florida rookery involved the release there of several thousand 1-year-old Tortuguero turtles during a restocking effort conducted from 1960 to 1971 (27). The success of this effort is unknown because most of the juveniles were released untagged, but it is possible that some of these turtles contributed to the nests that we sampled in 1987.

A third qualification to the conclusion of strict natal homing in green turtles concerns the comparison between the Tortuguero and Aves colonies. Turtles from these nesting beaches are known to share numerous foraging grounds in the Caribbean (Fig. 2). Among eight turtles from Aves tested, one exhibited the mtDNA genotype A that characterized all 15 Tortuguero samples (Table 1). These results yield an estimate of  $Nm = 0.5$ , with 95% confidence limit 0.0 to 2.1 (Table 2). Unless the A genotype has arisen more than once by a convergent mutation, its presence in both colonies must be due either to shared descent from an ancestral population (that is, symplesiomorphy) or to past or ongoing gene flow. Such gene flow could have resulted either from imperfect natal homing or occasional social facilitation.

This uncertainty raises a more general

**Table 2.** Above diagonal: results of  $2 \times 2$  tests of independence between mtDNA genotype and nesting locality for pairwise comparisons of the assayed green turtle rookeries, with the use of the G-statistic with Yates' correction for small sample size (29). In each test,  $df = 1$ , and probabilities ( $P$ ) are indicated. Below diagonal: estimates of  $Nm$  (and 95% confidence limits) for individual pairs of localities by the methods described (25, 26). Multiple comparisons used to calculate the individual pairwise values of  $Nm$  are not statistically independent. Abbreviation: NS, not significant.

	Aves	Tortuguero	Ascension	Florida
Aves		G = 8.1 ( $P < 0.005$ )	G = 11.2 ( $P < 0.005$ )	G = 6.2 ( $P < 0.05$ )
Tortuguero		$Nm = 0.5$ (0.0–2.1)	G = 17.0 ( $P < 0.005$ )	G = 0.0 (NS)
Ascension		$Nm = 0$ (0.0–0.4)	$Nm = 0$ (0.0–0.3)	G = 59.1 ( $P < 0.005$ )
Florida		$Nm = 0.5$ (0.0–2.1)		$Nm = 0$ (0.0–0.4)

issue concerning expectations of population genetic structure under the natal homing versus social facilitation hypotheses (Fig. 1). Unless natal homing is perfect (and social facilitation to nonnatal rookeries nonexistent), these two models of migratory behavior can converge with respect to predictions on magnitude of gene flow between nesting localities. In other words, occasional "mistakes" in natal homing, or occasional instances of social facilitation, or a combination, would lead to a sharing of genotypes between rookeries and to estimates of  $Nm > 0$  (as is true for Aves-Tortuguero). Thus, by hard criteria, our data cannot eliminate the possibility that occasional social facilitation may spread genotypes among proximal nesting localities. However, since the reciprocal exchange of even a single migrant per generation ( $Nm = 1$ ) should be sufficient to prevent the fixation or near fixation of different genotypes among rookeries, the highly significant genotype differences among green turtle rookeries in the Caribbean and Atlantic strongly suggest that natal homing predominates. We conclude that social facilitation to nonnatal sites must be rare.

Green turtles have colonized oceanic islands and mainland coasts in tropical regions around the world. Each colonization event involved at least one breakdown in fidelity to a nesting beach and clearly cannot be attributed to social facilitation. Thus, natal homing must be imperfect. However, the striking mtDNA population genetic structure among most nesting colonies indicates that maternal genetic exchange is quite rare. This discovery has an important bearing on conservation efforts. As noted by Carr (28), if turtle rookeries are genetically distinct, they are likely to be demographically independent. Protection afforded to one colony would not likely have an immediate impact on others, and consequently, management or recovery plans would have to be implemented on a rookery-specific basis.

#### REFERENCES AND NOTES

1. A. F. Carr, *So Excellent a Fish: A Natural History of Sea Turtles* (Scribner, New York, 1967; rev. ed., 1984); A. L. Koch, A. Carr, D. W. Ehrenfeld, *J. Theor. Biol.* **22**, 163 (1960).
2. G. H. Balazs, *U.S. Dep. Commer. NOAA Tech. Memo. Natl. Mar. Fish. Serv.*, NOAA-TM-NMFS-SWFC-36 (1983).
3. A. F. Carr and M. H. Carr, *Ecology* **53**, 425 (1972).
4. ———, A. B. Meylan, *Bull. Am. Mus. Nat. Hist.* **162**, 1 (1978).
5. G. R. Hughes, *Oceanogr. Res. Inst. (Durban) Invest. Rep.* **36**, 1 (1974).
6. C. J. Limpus, thesis, University of Queensland, St. Lucia, Queensland (1985).
7. J. P. Schulz, *Zool. Verh. (Leiden)* **143**, 1 (1975).
8. N. B. Frazer and L. M. Ehrhart, *Copeia* **1985**(1), 73 (1985).
9. J.-Y. LeGall and G. R. Hughes, *Amphib.-Reptilia* **8**, 277 (1987).

10. A. Kontos *et al.*, *Mar. Turtle Newsl.* **42**, 10 (1988).
11. J. R. Hendrickson, *Proc. Zool. Soc. London* **130**, 455 (1958).
12. D. W. Owens, M. A. Grassman, J. R. Hendrickson, *Herpetologica* **38**, 124 (1982).
13. C. Gremone and J. L. Gomez, *Isla de Aves como Área de Desove de la Tortuga Verde* (Fundación para la Defensa de la Naturaleza, Caracas, Venezuela, 1984).
14. J. A. Mortimer and A. Carr, *Copeia* **1987**(1), 103 (1987).
15. C. K. Dodd, *Brimleyana* **7**, 39 (1982).
16. J. C. Avise, *Philos. Trans. R. Soc. London Ser. B* **312**, 325 (1986).
17. J. C. Avise *et al.*, *Annu. Rev. Ecol. Syst.* **18**, 489 (1987).
18. C. Moritz, T. E. Dowling, W. M. Brown, *ibid.*, p. 269.
19. W. M. Brown, M. George, A. C. Wilson, *Proc. Natl. Acad. Sci. U.S.A.* **76**, 1967 (1979).
20. R. A. Lansman, R. O. Shadé, J. F. Shapira, J. C. Avise, *J. Mol. Evol.* **17**, 214 (1981).
21. B. W. Bowen, A. B. Meylan, J. C. Avise, *Proc. Natl. Acad. Sci. U.S.A.* **86**, 573 (1989).
22. W. M. Brown, *ibid.* **77**, 3605 (1980).
23. Nine additional endonucleases (Bam HI, Bgl I, Bgl II, Bst EII, Cla I, Kpn I, Pst I, Sac I, and Xba I) were also employed. Since each produced only zero or one mtDNA cut in our assays, they were uninformative and not included in the estimates of sequence divergence.
24. M. Nei and W.-H. Li, *Proc. Natl. Acad. Sci. U.S.A.* **76**, 5269 (1979).
25. M. Sliskin and W. P. Maddison, *Genetics* **123**, 603 (1989).
26. M. Sliskin, *ibid.* **121**, 609 (1989).
27. A. F. Carr, *Natl. Geogr. Mag.* **131**(6), 876 (1967).
28. ———, *Copeia* **1975**, 547 (1975).
29. R. R. Sokal and F. J. Rohlf, *Biometry* (Freeman, San Francisco, CA, 1969).
30. G. Medina and G. Sole, personal communication.
31. We thank C. Laguerre, G. Medina, J. Ross, and R. Witham for help obtaining samples. G. Medina and G. Sole furnished unpublished data on Aves Island. Permits or logistic support were provided by B. Campbell, D. Carr, C. Carson, G. Cruz, E. Possardt, J. Woody, the U.S. Air Force, and the Caribbean Conservation Corporation. We thank A. Huff, L. French, and J. Leiby for comments on the manuscript. Supported by the National Geographic Society and by NSF grants to B.W.B. and J.C.A.

22 December 1989; accepted 27 March 1990

## Cloning of a 67-kD Neutrophil Oxidase Factor with Similarity to a Noncatalytic Region of p60<sup>c-src</sup>

THOMAS L. LETO,\* KAREN J. LOMAX, BRYAN D. VOLPP, HIROYUKI NUNOI, JOAN M. G. SECHLER, WILLIAM M. NAUSEEF, ROBERT A. CLARK, JOHN I. GALLIN, HARRY L. MALECH

Chronic granulomatous diseases (CGDs) are characterized by recurrent infections resulting from impaired superoxide production by a phagocytic cell, nicotinamide adenine dinucleotide phosphate (reduced) (NADPH) oxidase. Complementary DNAs were cloned that encode the 67-kilodalton (kD) cytosolic oxidase factor (p67), which is deficient in 5% of CGD patients. Recombinant p67 (r-p67) partially restored NADPH oxidase activity to p67-deficient neutrophil cytosol from these patients. The p67 cDNA encodes a 526-amino acid protein with acidic middle and carboxyl-terminal domains that are similar to a sequence motif found in the noncatalytic domain of *src*-related tyrosine kinases. This motif was recently noted in phospholipase C-γ, nonerythroid α-spectrin (fodrin), p21<sup>ras</sup>-guanosine triphosphatase-activating protein (GAP), myosin-1 isoforms, yeast proteins cdc-25 and fus-1, and the 47-kD phagocyte oxidase factor (p47), which suggests the possibility of common regulatory features.

**C**Omplimentary DNAs encoding three oxidase components defective in distinct forms of CGD have been reported; two encode subunits of the membrane-bound cytochrome b-558 (1) and one encodes p47 phagocyte cytosolic oxidase factor (2, 3). Complementary DNA clones encoding the p67 cytosolic factor were obtained as described (2) by screening a Lambda-ZAP (Stratagene) expression library con-

taining cDNA inserts derived from HL60 cells differentiated for 2 days with dibutyryl adenosine 3',5'-monophosphate (dibutyryl cAMP). The library was screened with polyclonal rabbit antiserum B-1, which reacts against both p67 and p47 (4, 5). Several independent cDNA inserts encoding p67 were isolated, ranging in size from 2.2 to 0.5 kb (6).

To demonstrate that these clones encoded a protein antigenically similar to p67, we showed that fusion proteins encoded by two of the largest clones specifically blocked B-1 antibody detection of native p67 on SDS-polyacrylamide gel electrophoresis (SDS-PAGE) immunoblots of neutrophil cytosol (7). Furthermore, rabbit antibodies to r-p67 (8) reacted specifically against a 67-kD polypeptide in neutrophil cytosol from

T. L. Leto, K. J. Lomax, H. Nunoi, J. M. G. Sechler, J. I. Gallin, H. L. Malech, Bacterial Diseases Section, Laboratory of Clinical Investigation, National Institute of Allergy and Infectious Diseases, Building 10, Room 11N112, Bethesda, MD 20892.  
B. D. Volpp, W. M. Nauseef, R. A. Clark, Department of Medicine, University of Iowa and Veterans Administration Medical Center, Iowa City, IA 52242.

\*To whom correspondence should be addressed.

all normal subjects and most CGD patients except one who was previously characterized as p67-deficient (Fig. 1a). The p67 cDNA detected an ~2.4-kb mRNA transcript in monocytes from normal individuals and all CGD patients examined including the one patient with p67 protein deficiency (Fig. 1b). The p67 transcript was not detected in uninduced HL60 cells, but a transcript identical in size to that seen in monocytes was present in HL60 cells induced to differentiate with retinoic acid for 5 days, consistent with earlier observations indicating that p67 protein is limited to cells capable of superoxide generation (5).

Further evidence was sought to confirm that these cDNAs encode a functional factor absent from p67-deficient autosomal recessive CGD patients. This was accomplished by demonstrating that r-p67 is functionally active in a cell-free superoxide-generating assay requiring neutrophil membranes and cytosol (Fig. 2) (4, 9). The r-p67 partially reconstituted nicotinamide adenine dinucleotide phosphate (reduced) (NADPH)-dependent superoxide production by neutrophil cytosol from a p67-deficient CGD patient (Fig. 2b), but failed to restore activity to neutrophil cytosols from p47-deficient CGD patients (Fig. 2, c, d, and e). In control experiments oxidase activity was also partially restored when p47-deficient cytosols were mixed with the p67-deficient cytosol (Fig. 2f). Several factors account for the less than complete restoration, including lability of patient cytosol, presence of inhibitors in the *Escherichia coli*-derived r-p67 that diminish even normal cytosolic activity (Fig. 2a) and the inherent lability of r-p67 during isolation. (Less than maximal activity was seen in the complementation experiment in Fig. 2f.)

The nucleotide sequence of p67 cDNA (clone 10) predicts a 526-amino acid protein with a calculated size of 60,900 kD (Fig. 3a). The apparent size of the clone 10 recombinant fusion protein by SDS-PAGE was 70 kD (6, 7). A methionine codon occurs 25 bases from the 5' end of clone 10 cDNA within a consensus sequence that conforms to translation initiation sites observed in eukaryotic mRNAs (10). After a stop codon at position 1579, there are another 557 bases of untranslated sequence, which include two polyadenylation signals (underlined in Fig. 3a).

Within the predicted peptide sequence, the COOH-terminal domain was noted for a large number of acidic residues, bearing a net charge of -12 in the last 65-residue segment. Comparison of the deduced amino acid sequence of p67 with sequences recorded in the National Biomedical Research Foundation (NBRF) database (version 23)